Electronic Materials Letters (2023) 19:580–587
https://doi.org/10.1007/s13391-023-00427-2

ORIGINAL ARTICLE - NANOMATERIALS

Synthesis of CeO_2 Nanoparticles Derived by Urea Condensation for Chemical Mechanical Polishing

Zhenyang Wang[1] · Tongqing Wang[1] · Lifei Zhang[1] · Xinchun Lu[1]

Received: 29 January 2023 / Accepted: 17 March 2023 / Published online: 10 April 2023

Abstract

The synthesis of CeO_2 nanoparticles for CeO_2 based slurry gains continuous emphasis on improving its performance in the chemical mechanical polishing of dielectric materials. Urea was selected to dominate the growth and morphology during the calcination process. Thermogravimetry experiments were used to analyze the the decomposition behavior. Particle morphology and size were analyzed. Crystalline phase information and surface valence were used to compare the differences in surface physical and chemical properties of ceria by different synthesis process. The CeO_2 nanoparticles synthesized with urea were dispersed in water as slurry. The particle sizes of CeO_2 were measured by dynamic light scattering. The Zeta potential of CeO_2 dispersion were measured to show dispersing performance. The CeO_2 nanoparticles synthesized with urea condensation show good monodisperse properties. The material removal rate of silicon oxide and surface quality after chemical mechanical polishing were selected to evaluate the chemical mechanical polishing performance. The CeO_2 nanoparticles synthesized with urea condensation not only yielded better surface quality results than the commercial slurry but also showed a 153% (pH = 4) and 100% (pH = 10) increase in the material removal rate of silicon oxide compared to commercial.

Graphical Abstract

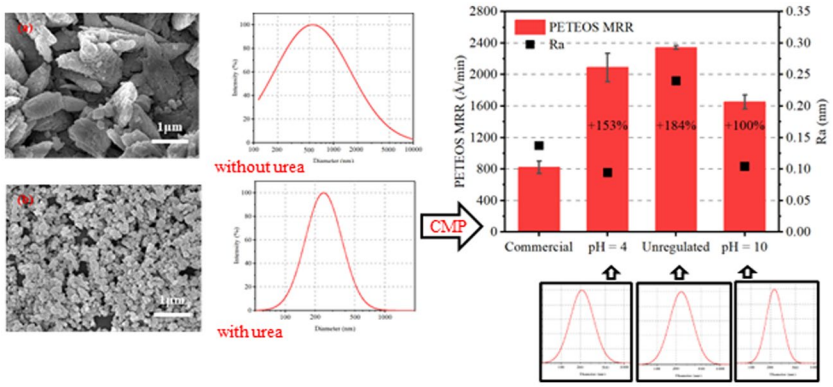

Keywords CeO_2 nanoparticles · Calcination synthesis · Urea condensation · Chemical mechanical polishing

1 Introduction

With the decreasing of critical dimension, Chemical Mechanical Polishing (CMP) has played an increasingly important role in integrated circuit fabrication. It is widely believed that slurry is one of the important CMP consumable materials [1]. In the logic chip manufacturing process, there are many dielectric CMP processes [2], such as Shallow Trench Isolation (STI), Inter-level Dielectric (ILD) and Ploy Silicon Open (POP) process, which need CeO_2 based

✉ Xinchun Lu
xclu@tsinghua.edu.cn

[1] State Key Laboratory of Tribology, Tsinghua University, Beijing 100084, China

slurry [3]. The synthesis [4] of CeO_2 nanoparticles in CeO_2 based slurry gains continuous emphasis on improving its performance in the CMP of dielectric materials.

The physical properties of CeO_2 nanoparticles in CeO_2 based slurry are significantly affected by the category and circumstance of synthesis [5]. The CMP performances of CeO_2 nanoparticles synthesized by different categories [6] and circumstances have been extensively investigated [7]. Calcination is a straightforward access to acquire CeO_2 nanoparticles [8]. Calcined CeO_2 has high SiO_2 Material Removal Rate (MRR) [9] and good within-wafer uniformity [7]. Previous studies [10] have shown that the higher the calcination temperature, the higher the CMP MRR of ceria [11]. Ceria calcined at 900 ℃ has the highest MRR [12]. However, calcined CeO_2 is prone to sintering and agglomeration at high calcination temperatures [13]. In general, calcined CeO_2 usually requires subsequent milling processes [14] to achieve the desired size [15], which consumes considerable energy [16]. Therefore, a new method that can prevent agglomeration during the calcination of ceria particle must be proposed.

In this work, urea was selected to dominate the growth of particle during the calcination process. Therefore, the findings in the manuscript provide the correlation between the growth state of CeO_2 nanoparticles and the calcination process controlled by urea [17]. In addition, the dispersion and CMP performance of the CeO_2 nanoparticles were measured.

2 Experimental Procedure

2.1 Synthesis of Materials

Calcination thermal decomposition was a common and widespread process to synthesize CeO_2. In this research, $Ce_2(CO_3)_3{\cdot}6H_2O$ was used as the source of ceria.

Urea and $Ce_2(CO_3)_3{\cdot}6H_2O$ were mixed as a 1:1 molar ratio to get a uniform paste. The other was prepared without urea. The paste was exsiccated to solid under a constant temperature oil bath condition at 70 ℃. The solid was calcined in muffle furnace at 900 ℃ with a heating rate at 10 °C/min, maintained at a constant temperature for 10 h and then naturally cooled down to room temperature. The process of the synthesis of CeO_2 nanoparticles with urea is shown in Fig. 1. The decomposition behavior of two kinds of exsiccated solid was monitored by thermal gravimetric apparatus (TGA/DSC1, Mettler Toledo) up to 900 ℃ at a heating rate of 10 °C/min in air.

2.2 Materials Characterization

The size and morphology of CeO_2 were observed by scanning electron microscopy (SEM, SU8200, Hitachi). The lattice structure and grain size were analyzed by the X-ray diffraction (XRD, D/max-2550, Rigaku) using a Cu-Kα X-ray source (40 kV, 40 mA) in the range of 20–90°.

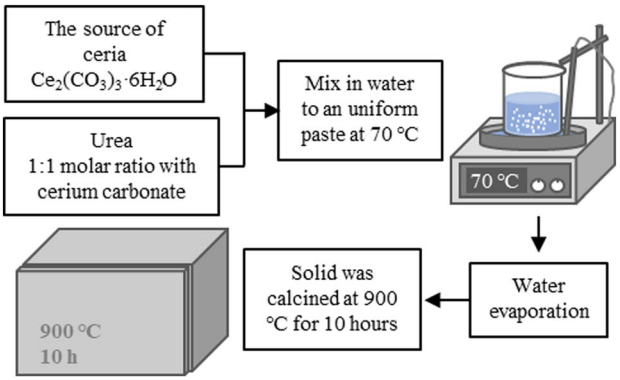

Fig. 1 Flow chart of the synthesis of CeO_2 nanoparticles with urea

The valence states of cerium were carried out using X-ray photoelectron spectroscopy (XPS, PHI Quantera II, Ulvac-Phi). The fraction of Ce^{3+} was calculated based on the deconvolution [18] of Ce 3d spin-orbit doublet using Casa XPS.

2.3 CMP Process

CeO_2 nanoparticles calcined with urea were dispersed in deionized water, the mass content of the dispersion was 0.3%, and the pH of the dispersion was adjusted by nitric acid and ammonia [19]. The CeO_2 dispersions were prepared by continuous ultrasonication and stirring for 10 h.

The particle size of dispersed CeO_2 nanoparticles was measured by a laser particle size analyzer (380ZLS, PSS). The Zeta potential of dispersed CeO_2 nanoparticles was measured by a zeta potential analyzer (90Plus PALS, Brookhaven).

50 mm Plasma-Enhanced Tetraethyl Orthosilicate (PETEOS) silicon oxide wafers were prepared by SKW Associates, Inc. for CMP process. The thicknesses of the as-deposited oxide were 10 kA. Wafers were polished on a CMP machine (Universal-150Plus, Hwatsing) with a CMP pad (DH3010, Dinglong). Ex-situ conditioning was carried out with a diamond dresser (A165, 3 M) before each polishing. The head/platen rotational speed was 87/93 rpm, the slurry flow rate was 150 ml/min, and the down pressure was 3 psi. The main polishing time is 60 s. The commercial slurry for comparison is Ces333F from AGC.

The MRR of CMP process was calculated by the thickness difference of wafers [20] before and after CMP process that were measured by by Filmetrics (F50, Filmetric). The surface quality after CMP process was observed by atomic force microscope (AFM, Icon, Bruker). The average roughness (Ra) was determined within $2.0 \times 2.0\ \mu m^2$.

3 Results and Discussion

3.1 Surface Morphology of CeO_2 Nanoparticles

The SEM images of the CeO_2 nanoparticles are shown in Fig. 2, which provide the information of particle morphology. The shape of the CeO_2 nanoparticles synthesized with urea is near-spherical and shows good monodisperse properties.

It is clear that the particle sizes of the two kinds of CeO_2 are around 60 nm. CeO_2 nanoparticles synthesized without urea are obviously agglomerated to form a strip particle combination. CeO_2 usually has a strong precursor inheritance during the calcination process, so the strip particle combination is likely to be the morphology of cerium carbonate [21].

However, when urea is involved in the calcination process, the growth and combination of CeO_2 nanoparticles are significantly changed. This phenomenon can be attributed to the thermal condensation reaction of urea [22]. The condensation reaction of urea occurs in the two-way reaction of dissolution and precipitation of cerium carbonate. The condensation product has a template effect so that CeO_2 nanoparticles can grow in a monodisperse form [23].

The results of thermogravimetry experiments are shown in Fig. 3, which could reflect the changes of phase in the calcination process. In the TG curve of the calcination process without urea, the low weight loss within lower temperature range (≤ 100 °C) indicates that there is no loss of crystal water in the process. This result shows that the exsiccation process at 70 °C was sufficient. The rapid weight loss from 240 to 290 °C indicates that cerium carbonate was rapidly decomposed. The TG curve of the calcination process with urea is more complex. The slow weight loss begins at 80 °C, which could be explained that urea began to react. Subsequently, the decline rate of the curve changed at 240 °C. Cerium carbonate began to decompose. Contrary to the previous rapid decline, the decomposition of cerium carbonate gradually completed with the increase of temperature. This result shows that the decomposition of cerium

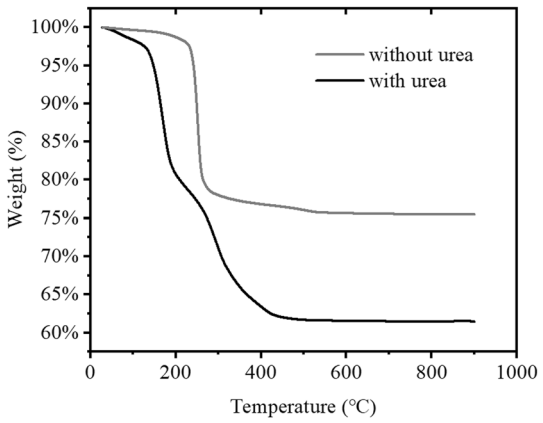

Fig. 3 Thermogravimetry (TG) curves of CeO_2 nanoparticles synthesized with urea and without urea

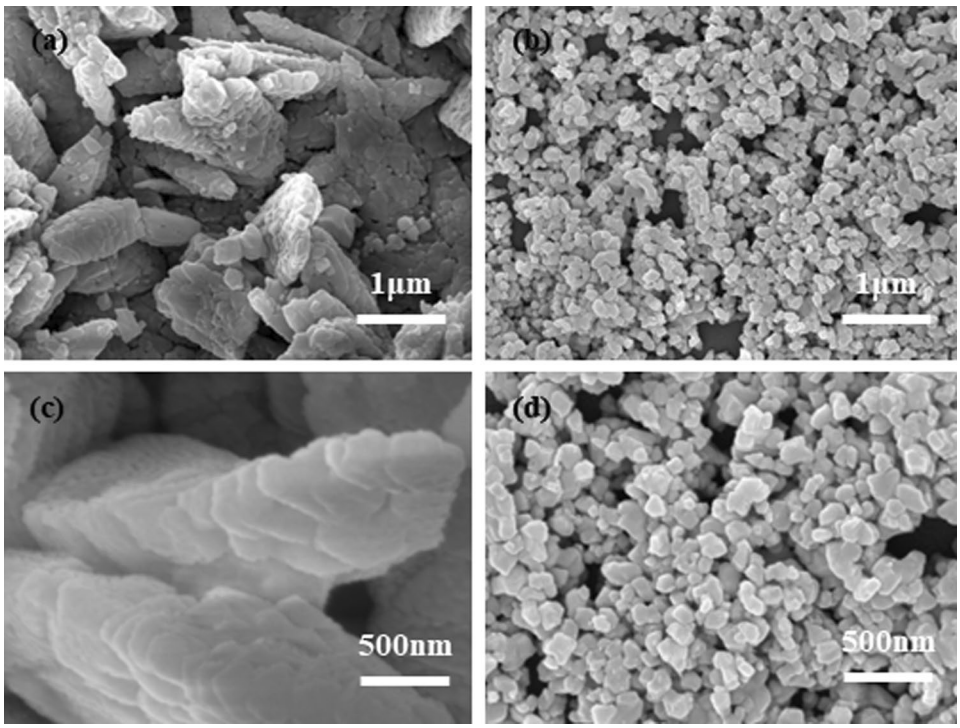

Fig. 2 SEM images of CeO_2 nanoparticles synthesized (**a**), (**c**) without urea and (**b**), (**d**) with urea

Table 1 The concentration of Ce^{3+} of CeO_2 Synthesized with and without urea

	With urea	Without urea
The concentration of Ce^{3+}	16.90%	16.27%
Crystallinity	97.70%	99.31%
Crystallite size (nm)	62.2	62.5

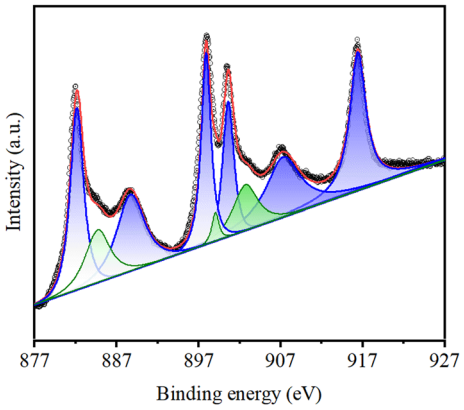

Fig. 4 XPS spectra of CeO_2 nanoparticles synthesized without urea

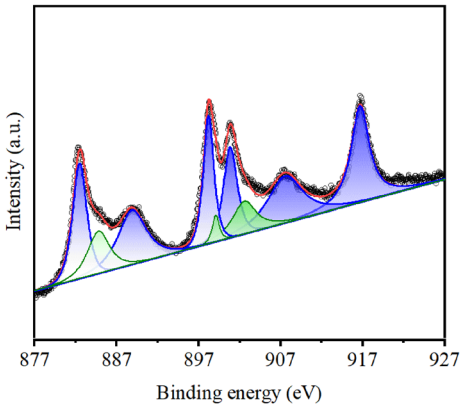

Fig. 5 XPS spectra of CeO_2 nanoparticles synthesized with urea

carbonate and the growth of CeO_2 were affected by urea condensation products.

3.2 Surface and Structural Properties

XPS spectra in Figs. 4 and 5 show the difference of the concentration of Ce^{3+} between two kinds of CeO_2 nanoparticles. Table 1 shows the concentration of Ce^{3+} in the CeO_2 nanoparticles conducted by peak deconvolution of XPS spectra [24].

Figure 6 shows the crystalline phase information of the CeO_2 nanoparticles synthesized without urea and with urea by XRD. The XRD patterns of CeO_2 nanoparticles remain

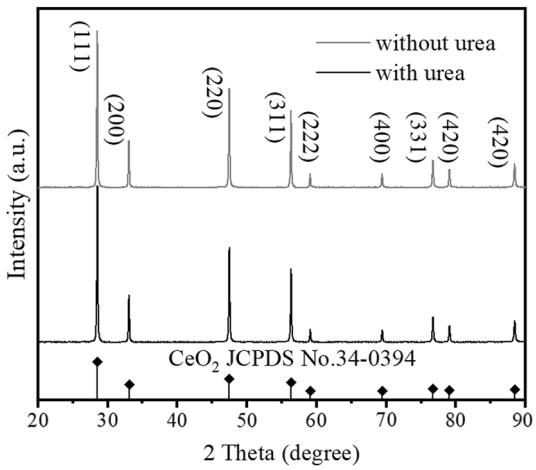

Fig. 6 XRD patterns of CeO_2 nanoparticles synthesized with urea and without urea

the typical pattern of fluorite structure and correspond well with the standard data of JCPDS No. 34-0394 [25]. According to the Debye-Scherrer equation, the crystallite size could be calculated based on the broadening of the diffraction peak and the Bragg angle [26].

There are almost no differences in the concentration of Ce^{3+} and crystallite size between the two kinds of CeO_2 nanoparticles. Because of the presence of urea, the crystallinity of the product decreased slightly. However, urea condensation could not change the surface and structural properties of CeO_2 nanoparticles. This result further confirms that the urea condensation reaction only acts as a physical template. The CeO_2 nanoparticles synthesized with urea have the similar physical and chemical properties to general calcined ceria.

3.3 CMP Performance

Figure 7 compares the particle size of the two kinds of CeO_2 nanoparticles with different pH measured by dynamic light scattering [27]. Figure 7a shows that the mean diameter of CeO_2 nanoparticles synthesized without urea is approximately 600 nm with a wide distribution range.

Figure 7b–d show that the CeO_2 nanoparticles synthesized with urea have good dispersion. Simultaneously, the particle size had good stability and did not fluctuate greatly with the change of pH value [28]. Table 2 shows the standard deviation of DLS particle sizes. Compared with the initial particle size without regulating pH, the mean diameter was smaller and the particle size distribution was more concentrated at pH = 4 and pH = 10. Table 2 also shows the Zeta potential of CeO_2 dispersion prepared by nanoparticles synthesized with urea at different pH value. This result is consistent with the results of

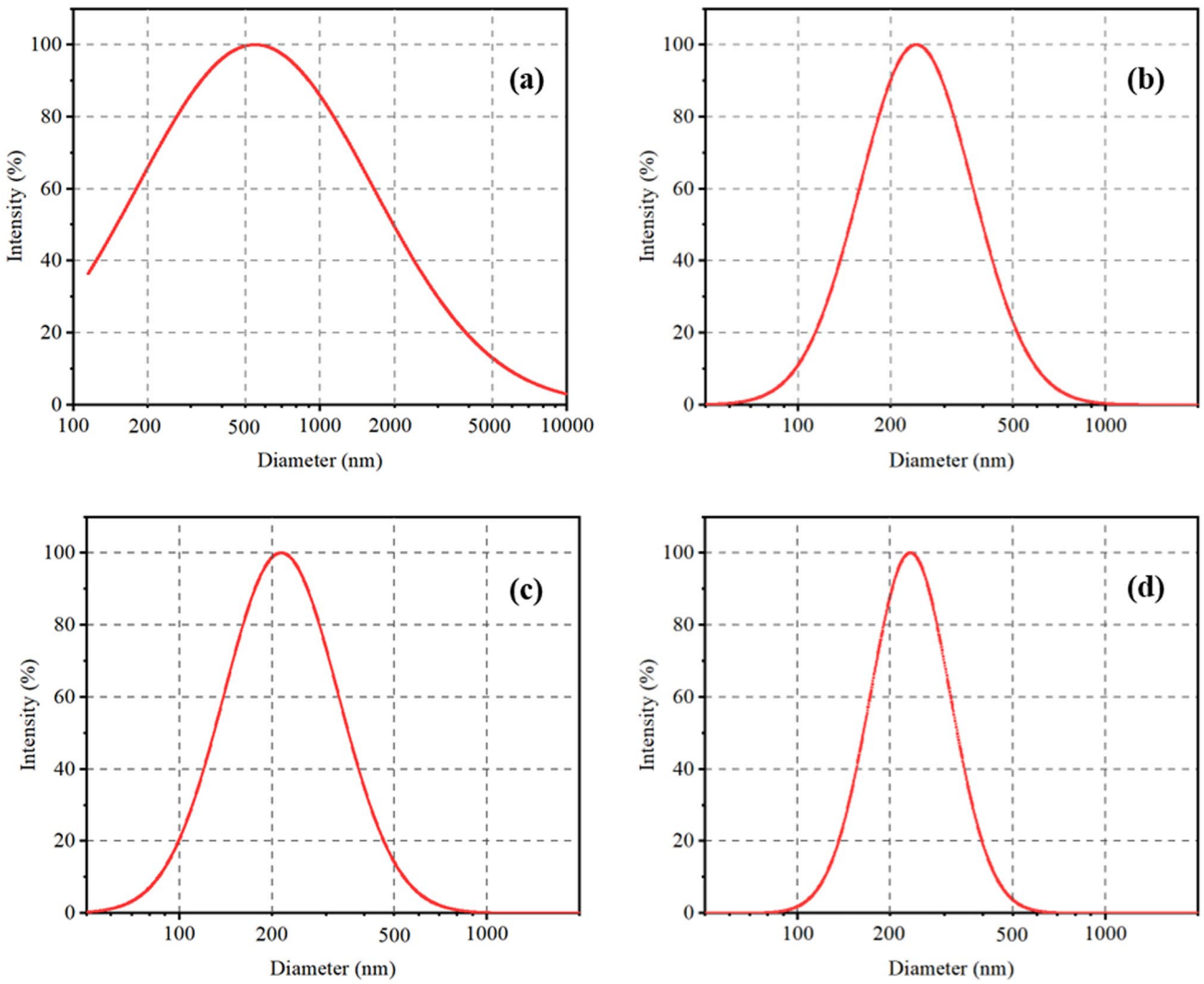

Fig. 7 DLS particle sizes of CeO_2 nanoparticles synthesized (**a**) without urea and (**b**) with urea dispersed in water; synthesized with urea dispersed in water at (**c**) pH = 4 and (**d**) pH = 10

Table 2 The DLS particle size and Zeta potential of CeO_2 dispersion synthesized with urea

	pH = 4	Unregulated	pH = 10
Mean diameter (nm)	235.3	265.7	243
Standard deviation	100.9	111.8	75.8
Zeta potential (mV)	32.66	−12.79	−23.29

previous studies on CeO_2 dispersions. Meanwhile, when the pH is not regulated, that is, the pH is close to the isoelectric point of ceria, the absolute value of Zeta potential of CeO_2 dispersion is lower and the dispersion is slightly worse, which also corresponds to the increase of mean particle size. This phenomenon indicates that the CeO_2 nanoparticles synthesized with urea could be used as a

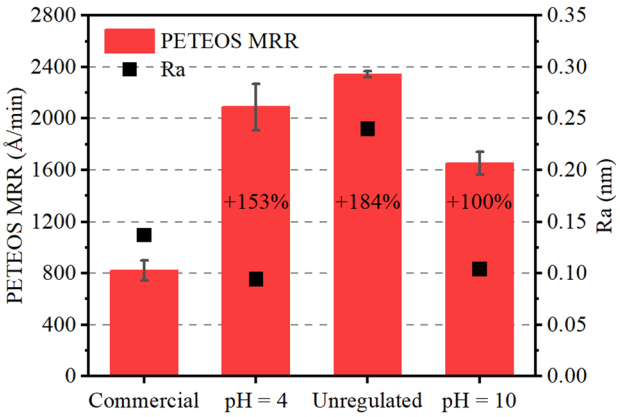

Fig. 8 MRR of PETEOS during CMP and surface roughness after CMP by using CeO_2 nanoparticles synthesized with urea dispersed in water at different pH value compared with commercial slurry

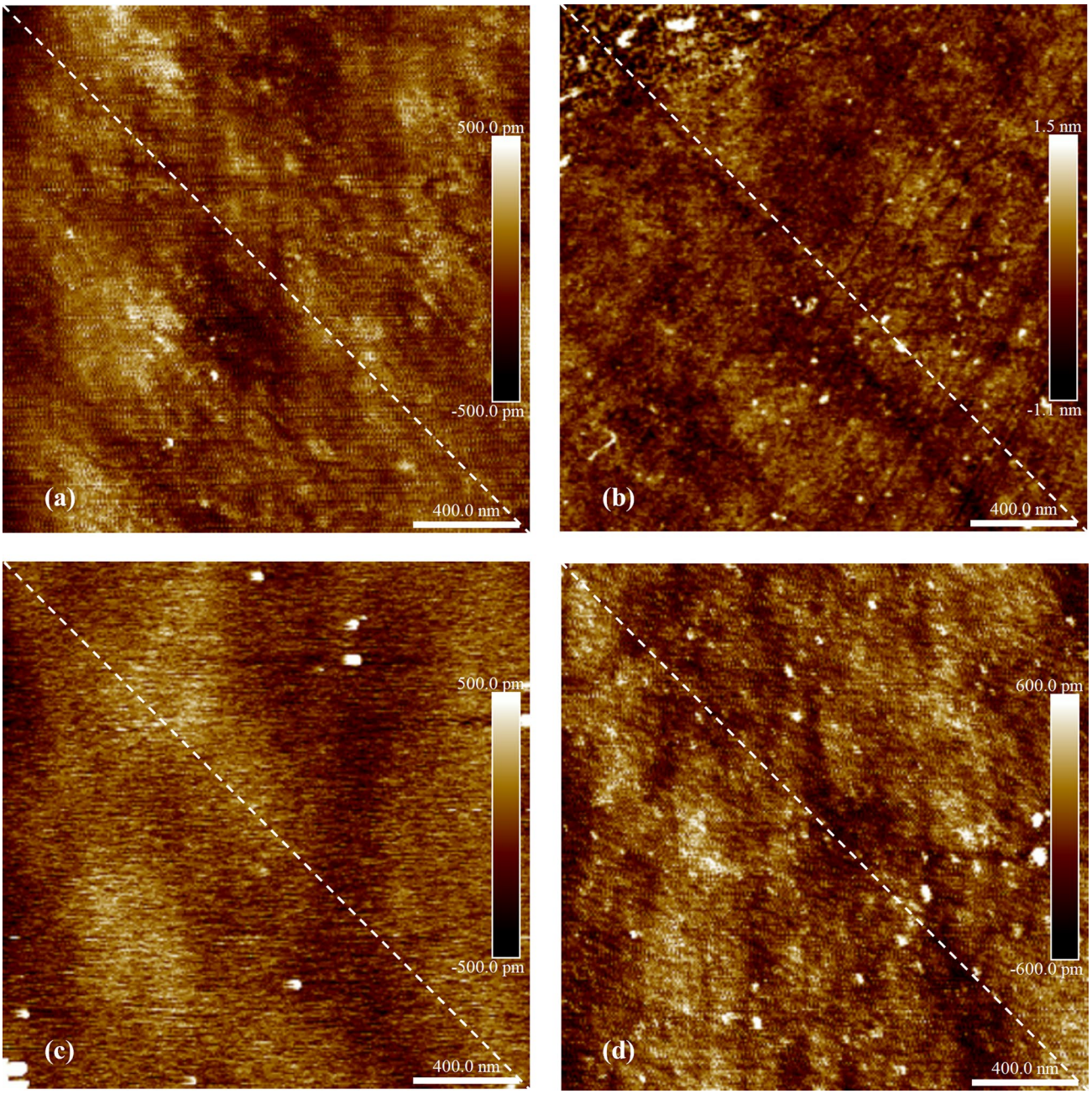

Fig. 9 2D-AFM height images of surfaces after CMP process by using CeO_2 nanoparticles synthesized with urea dispersed in water at (**a**) pH = 4, (**b**) unregulated pH and (**c**) pH = 10, compared with using (**d**) commercial slurry

good basic material for the subsequent development of multifunctional CMP slurry [29].

The MRR of PETEOS of CMP experiments are shown in Fig. 8. The initial ceria without regulating pH showed a higher MRR because of the bigger mean diameter. The MRR of PETEOS was higher in acidic slurry (at pH 4) than that in alkaline slurry (at pH 10), mainly due to the different electrostatic interactions between abrasive and the wafer surface [30]. Three kinds of slurries all exhibited higher MRR than commercial slurry.

The micro topographies after CMP process observed by AFM are shown in Figs. 9 and 10. AFM results clearly reveal that CMP process using the CeO_2 dispersion prepared by nanoparticles synthesized with urea achieve ultra-smooth and damage-free surfaces.

The surface roughness (Ra) results after CMP process are shown in Fig. 8. The CeO_2 dispersion prepared by

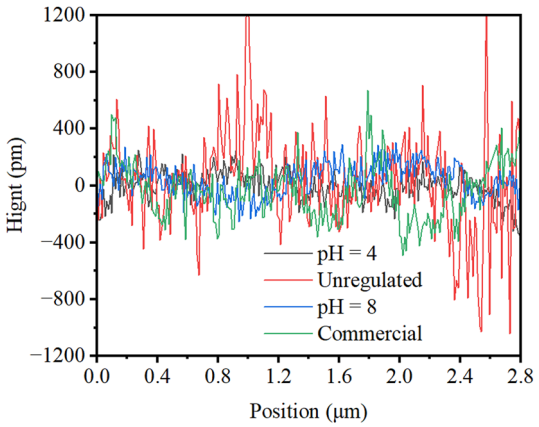

Fig. 10 The line-scan profiles of surfaces corresponding to the 2D-AFM height images of surfaces after CMP process in Fig. 9

nanoparticles synthesized with urea at unregulated pH has a relatively poor surface quality due to the lower absolute value of Zeta potential and larger particle size. Compared with commercial slurry, acidic slurry (at pH 4) and alkaline slurry (at pH 10) both have a better surface quality.

These CMP results also increase the possibility of subsequent development of multifunctional CMP slurry.

4 Conclusions

Urea was selected to dominate the growth and morphology during the calcination process. The urea condensation products made the calcined CeO_2 exhibit good monodisperse characteristics by affecting the decomposition of cerium carbonate and the growth of CeO_2. At the same time, the urea condensation reaction did not affect the crystal structure and surface properties of the calcined CeO_2. The CeO_2 nanoparticles synthesized with urea condensation had good dispersion in water at a wide pH value and satisfactory CMP performance. The CeO_2 nanoparticles synthesized with urea condensation not only yielded better surface quality results than the commercial slurry but also showed a 153% (pH = 4) and 100% (pH = 10) increase in the material removal rate of silicon oxide compared to commercial. The result of this research greatly reduces the energy consumption and time in the synthesis of calcined CeO_2 slurry. This research provides a broad prospect for the subsequent development of CMP slurry.

Acknowledgements This work was supported by the National Natural Science Foundation of China (No. 51991370).

Declarations

The authors declare that they have no known competing financial interests or personal relationships that could have appeared to influence the work reported in this paper.

References

1. Choe, J.H., et al.: Determination of particle size distribution in oxide Abrasive Slurry after chemical mechanical polishing process using Raman spectroscopy. Electron. Mater. Lett (2023). https://doi.org/10.1007/s13391-022-00401-4
2. Krishnan, M., et al.: Chemical mechanical planarization: slurry chemistry, materials, and mechanisms. Chem. Rev. (2010). https://doi.org/10.1021/cr900170z
3. Seo, J., et al.: Perspective—recent advances and thoughts on Ceria particle applications in chemical mechanical planarization. ECS J. Solid State Sci. Technol. (2022). https://doi.org/10.1149/2162-8777/ac8310
4. Abdullah, A., et al.: Comparative study of nano crystalline Ceria synthesized by different wet-chemical methods. J. Supercond. Novel Magn. (2014). https://doi.org/10.1007/s10948-013-2261-x
5. Kim, D.H.R.: Effect of calcination process on synthesis of Ceria particles, and its influence on shallow trench isolation chemical mechanical planarization performance. Jpn. J. Appl. Phys. (2006). https://doi.org/10.1143/JJAP.45.4893
6. Li, Y., et al.: Changing the calcination temperature to tune the microstructure and polishing properties of ceria octahedrons. RSC Adv. (2022). https://doi.org/10.1039/D2RA02367A
7. Srinivasan, R., et al.: Shallow trench isolation chemical mechanical planarization: a review. ECS J. Solid State Sci. Technol. (2015). https://doi.org/10.1149/2.0071511jss
8. Cao, X.F., et al.: Fabrication and application of CeO2 nanostructure with different morphologies: a review. J. Renew. Mater . (2020). https://doi.org/10.32604/jrm.2020.012113
9. Han, S., et al.: Effect of pad surface roughness on material removal rate in chemical mechanical polishing using ultrafine colloidal ceria slurry. Electron. Mater. Lett. (2013). https://doi.org/10.1007/s13391-012-2144-5
10. Kim, S.K., et al.: Influence of physical characteristics of Ceria particles on polishing rate of chemical mechanical planarization for shallow trench isolation. Jpn. J. Appl. Phys. (2004). https://doi.org/10.1143/JJAP.43.7427
11. Li, Y.X., et al.: Changing the calcination temperature to tune the microstructure and polishing properties of ceria octahedrons. RSC Adv. (2022). https://doi.org/10.1039/d2ra02367a
12. Oh, M.H., et al.: Polishing behaviors of ceria abrasives on silicon dioxide and silicon nitride CMP. Powder Technol. (2011). https://doi.org/10.1016/j.powtec.2010.09.025
13. Hyun-Goo, K., et al.: Effects of grain size and abrasive size of polycrystalline nano-particle ceria slurry on shallow trench isolation chemical mechanical polishing. Jpn. J. Appl. Phys. (2004). https://doi.org/10.1143/jjap.43.L365
14. Yadav, T.P., Srivastava, O.N.: Synthesis of nanocrystalline cerium oxide by high energy ball milling. Ceram. Int. (2012). https://doi.org/10.1016/j.ceramint.2012.04.025
15. Kim, S.K., et al.: Influence of crystalline structure of ceria on the remaining particles in the STI CMP. J. Electrochem. Soc. (2007). https://doi.org/10.1149/1.2735923
16. Varinot, C., et al.: Identification of the fragmentation mechanisms in wet-phase fine grinding in a stirred bead mill. Chem. Eng. Sci. (1997). https://doi.org/10.1016/S0009-2509(97)89693-5
17. Ratnayake, S.P., et al.: Low-temperature thermocatalytic particulate carbon decomposition via urea solution-combustion

derived CeO2 nanostructures. J. Rare Earths. (2021). https://doi.org/10.1016/j.jre.2020.02.013
18. Chahal, S., et al.: Electronic structure and photocatalytic activity of samarium doped cerium oxide nanoparticles for hazardous rose bengal dye degradation. Vacuum (2020). https://doi.org/10.1016/j.vacuum.2019.109075
19. Suphantharida, P., Osseo-Asare, K.: Cerium oxide slurries in CMP. Electrophoretic mobility and adsorption investigations of Ceria/Silicate interaction. J. Electrochem. Soc. (2004). https://doi.org/10.1149/1.1785793
20. Cheng, J., et al.: RE (La, nd and yb) doped CeO2 abrasive particles for chemical mechanical polishing of dielectric materials: experimental and computational analysis. Appl. Surf. Sci. (2020). https://doi.org/10.1016/j.apsusc.2019.144668
21. Sun, C., et al.: Nanostructured ceria-based materials: synthesis, properties, and applications. Energy Environ. Sci. (2012). https://doi.org/10.1039/C2EE22310D
22. Chidhambaram, N., Ravichandran, K.: Single step transformation of urea into metal-free g-C3N4 nanoflakes for visible light photocatalytic applications. Mater. Lett. (2017). https://doi.org/10.1016/j.matlet.2017.07.040
23. Zhang, Y., et al.: Porous graphitic carbon nitride synthesized via direct polymerization of urea for efficient sunlight-driven photocatalytic hydrogen production. Nanoscale (2012). https://doi.org/10.1039/c2nr30948c
24. Kim, E., et al.: Effects of trivalent lanthanide (La and nd) doped ceria abrasives on chemical mechanical polishing. Powder Technol. (2022). https://doi.org/10.1016/j.powtec.2021.11.069
25. Seo, J., et al.: Role of the oxidation state of cerium on the ceria surfaces for silicate adsorption. Appl. Surf. Sci. (2016). https://doi.org/10.1016/j.apsusc.2016.06.193
26. Kim, N.Y., et al.: A nanoclustered ceria abrasives with low crystallinity and high Ce3+/Ce4 + ratio for scratch reduction and high oxide removal rates in the chemical mechanical planarization. J. Mater. Sci. (2022). https://doi.org/10.1007/s10853-022-07338-x
27. Seo, J.: A review on chemical and mechanical phenomena at the wafer interface during chemical mechanical planarization. J. Mater. Res. (2021). https://doi.org/10.1557/s43578-020-00060-x
28. Abiade, J.T., et al.: Effect of pH on ceria–silica interactions during chemical mechanical polishing. J. Mater. Res. (2005). https://doi.org/10.1557/JMR.2005.0176
29. Pyo, S.G., et al.: Investigating the planarization behavior of high selective slurry with initial step height and pattern density. Electrochem. Solid State Lett. (2009). https://doi.org/10.1149/1.3117246
30. Kim, S., et al.: Adsorption behavior of anionic polyelectrolyte for chemical mechanical polishing (CMP). J. Colloid Interface Sci. (2008). https://doi.org/10.1016/j.jcis.2007.11.004